

## Supporting information

### Electrochemical Synthesis of Ammonia from Nitrogen Catalyzed by CoMoO<sub>4</sub> Nanorods under Ambient Conditions

Yizhen Zhang,<sup>a,d</sup> Jue Hu,<sup>b,\*</sup> Chengxu Zhang,<sup>c,\*</sup> Qianglong Qi,<sup>b</sup> Shanxiong Luo,<sup>c</sup>

Keda Chen,<sup>a</sup> Lifen Liu,<sup>d</sup> Michael K. H. Leung,<sup>a,\*</sup>

<sup>a</sup>Ability R&D Energy Research Centre, School of Energy and Environment, City

University of Hong Kong, Hong Kong, China

<sup>b</sup>Faculty of Science, Kunming University of Science and Technology, Kunming, China

<sup>c</sup>The Engineering Laboratory of Advanced Battery and Materials of Yunnan Province,  
Faculty of Metallurgical and Energy Engineering, Kunming University of Science and  
Technology, Kunming, China

<sup>d</sup>Key Laboratory of Industrial Ecology and Environmental Engineering (MOE), School  
of Environmental Science and Technology, Dalian University of Technology, Dalian,  
China

\*Corresponding author.

E-mail addresses: [hujue@kust.edu.cn](mailto:hujue@kust.edu.cn) (J. Hu), [chxzhang@kust.edu.cn](mailto:chxzhang@kust.edu.cn) (C. Zhang),  
[mkh.leung@cityu.edu.hk](mailto:mkh.leung@cityu.edu.hk) (M. Leung)

## Detection of ammonia

The indophenol blue method was adopted to determine the concentration of produced ammonia in aqueous solution via UV-vis spectrophotometry<sup>1</sup>. Three chromogenic reagents were prepared: solution A (1 M NaOH solution containing 5 wt% salicylic acid and 5 wt% sodium citrate), solution B (0.05 M sodium hypochlorite), and solution C (1 wt% sodium nitroferricyanide). Exactly 2 mL of standard solutions or sample solutions from the post-electrolysis electrolyte was mixed with 2 mL of solution A, 1 mL of solution B and 0.2 mL of catalyzing reagent C. After keeping for 2 h, the absorption spectrum of the resulting solution was measured using a UV-vis spectrophotometer within a wavelength range of 550 nm to 800 nm. The absorbance intensity at 665 nm was utilized to confirm the yield of ammonia on the basis of the standard curve. The standard curve was drawn by plotting the absorbance values with a series of concentrations for standard NH<sub>4</sub>Cl solution (from 0 to 50 μM in 0.1 M Na<sub>2</sub>SO<sub>4</sub> or 1 mM H<sub>2</sub>SO<sub>4</sub>). In Fig. S1, the fitting curves obtained a good linear relation between absorbance and NH<sub>3</sub> concentration ( $y_{\text{Na}_2\text{SO}_4} = 0.01683 + 0.00574x$ ,  $R_{\text{Na}_2\text{SO}_4}^2 = 0.9996$ ;  $y_{\text{H}_2\text{SO}_4} = 0.0144 + 0.0057x$ ,  $R_{\text{H}_2\text{SO}_4}^2 = 0.9993$ ).

The concentration of the probable by-product hydrazine (N<sub>2</sub>H<sub>4</sub>) was spectrophotometrically determined using the Watt and Chrisp method<sup>2</sup>. A mixture of 0.599 g para-(dimethylamino) benzaldehyde, 3 mL HCl (concentrated), and 30 mL ethanol was used as a color reagent. Exactly 3 mL of standard solutions or sample solutions from the post-electrolysis electrolyte and 0.5 mL of the color reagent were mixed and then kept in the dark for 15 min. The absorption spectrum of the resulting solution was measured using a UV-vis spectrophotometer within a wavelength range of 400 nm to 550 nm. The amount of formed N<sub>2</sub>H<sub>4</sub> was determined on the basis of absorbance intensity at 455 nm.

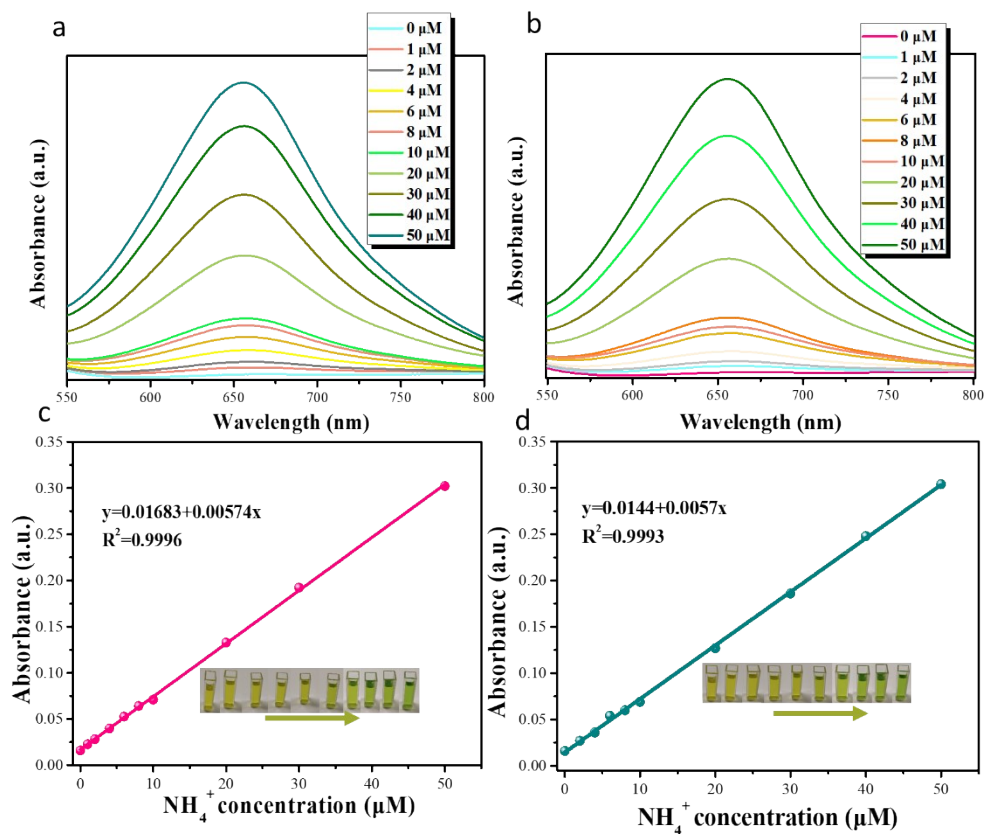


Figure S1 UV-vis curves of indophenol assays after being incubated for 2 h in (a) 0.1 M Na<sub>2</sub>SO<sub>4</sub> and (b) 1 mM H<sub>2</sub>SO<sub>4</sub>, calibration curves used for estimation of NH<sub>3</sub> concentration in (c) 0.1 M Na<sub>2</sub>SO<sub>4</sub> and (d) 1 mM H<sub>2</sub>SO<sub>4</sub> (Insert picture is the chromogenic reaction solution with indophenol indicator of increased NH<sub>4</sub><sup>+</sup> concentration)<sup>1</sup>.

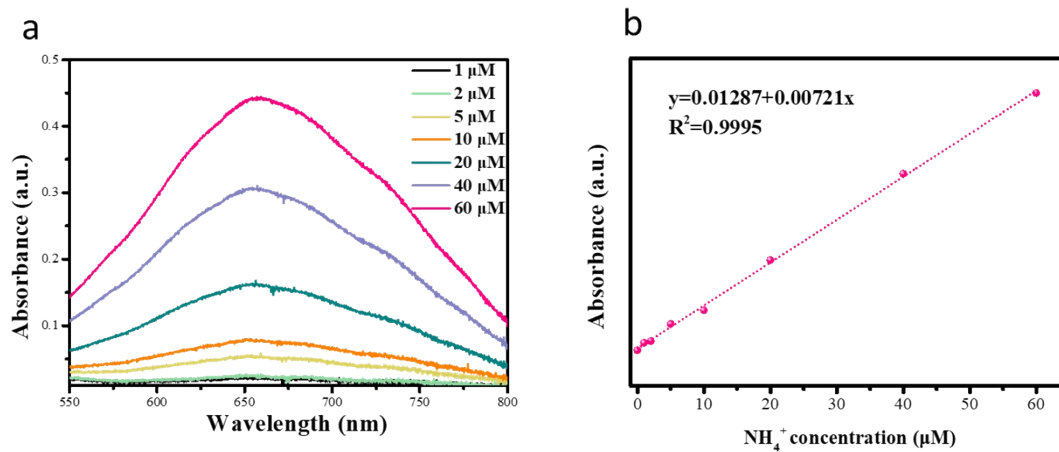


Figure S2 (a) UV-vis spectroscopy of indophenol assays after being incubated for 2 h in 0.1 M KOH solution and (b) the corresponding calibration curves used for estimation of  $\text{NH}_3$  concentration <sup>1</sup>.

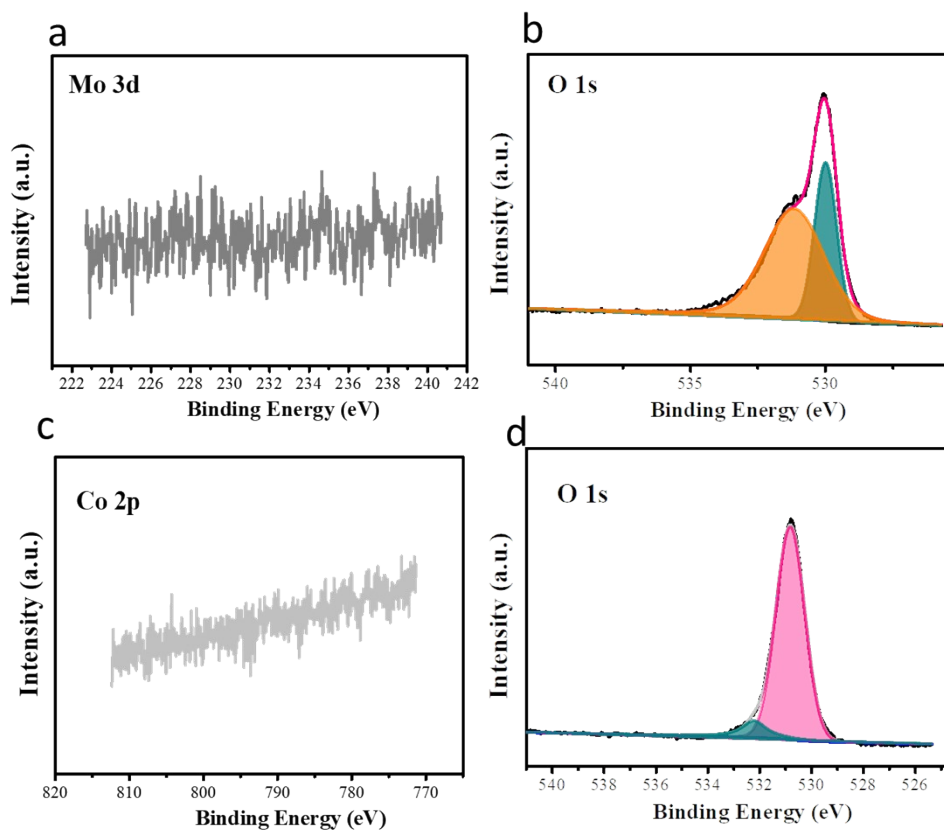


Figure S3 XPS spectra of CO-NR in the (a) Mo 3d and (b) O 1s regions, and MO-NR in the (c) Co 2p, (d) O 1s regions.

For CO-NR, there was no intensity of Mo 3d spectra in CO-NR (Figure S3a), because of the absence of Mo species. Two different peaks of O1s region (Figure S3b) were assigned to the lattice oxygen and surface adsorbed water or hydroxide species for CoO. As shown in Figure S3c, there was no signal of Co 2p spectra in MO-NR. The O 1s region of MO-NR was corresponding to the Mo–O and surface adsorbed water or hydroxide, respectively (Figure S3d).

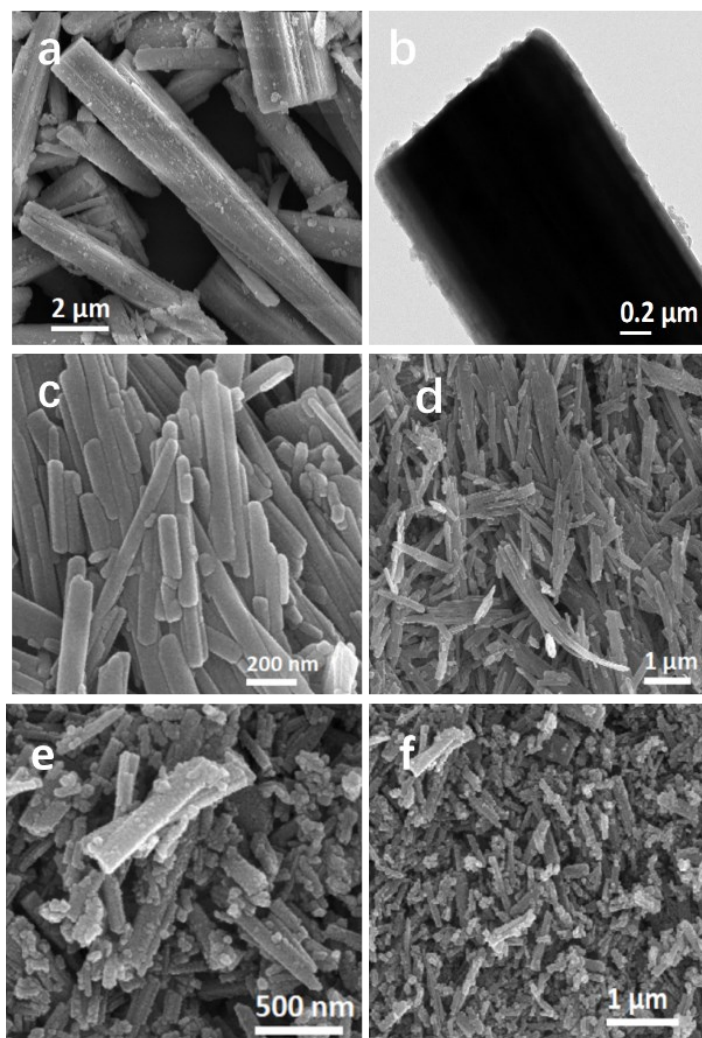


Figure S4 (a) SEM and (b) TEM images of CMO-NR; SEM images of (c-d) MO-NR and (e-f) CO-NR.

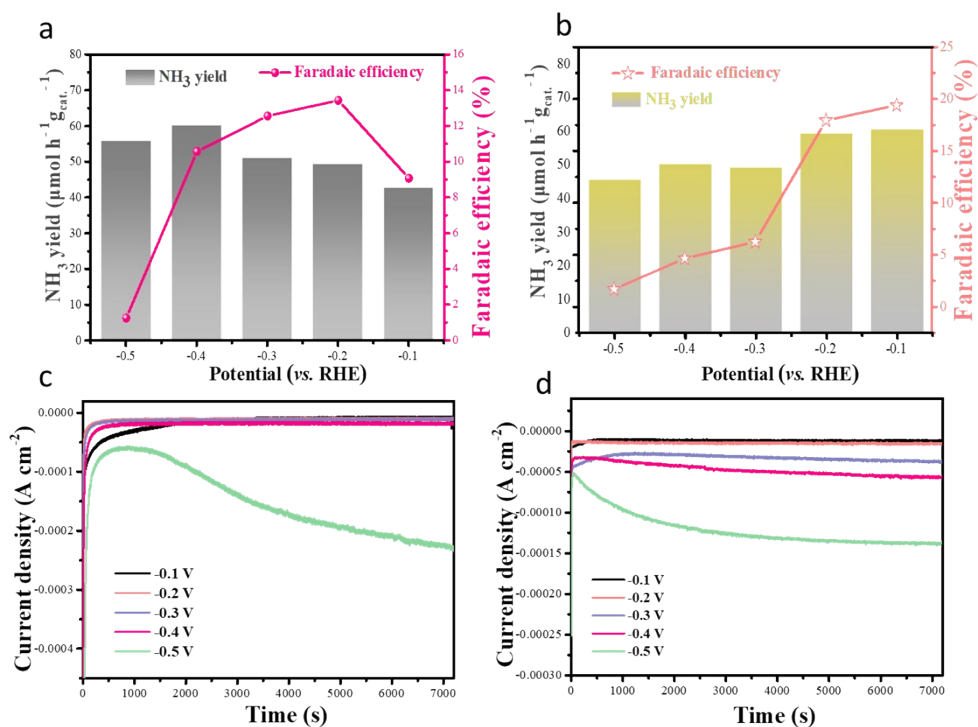


Figure S5  $\text{NH}_3$  yield rate and FEs of (a) CO-NR and (b) MO-NR, and corresponding CA results of (c) CO-NR and (d) MO-NR during 2 h electrolysis under the applied potentials.

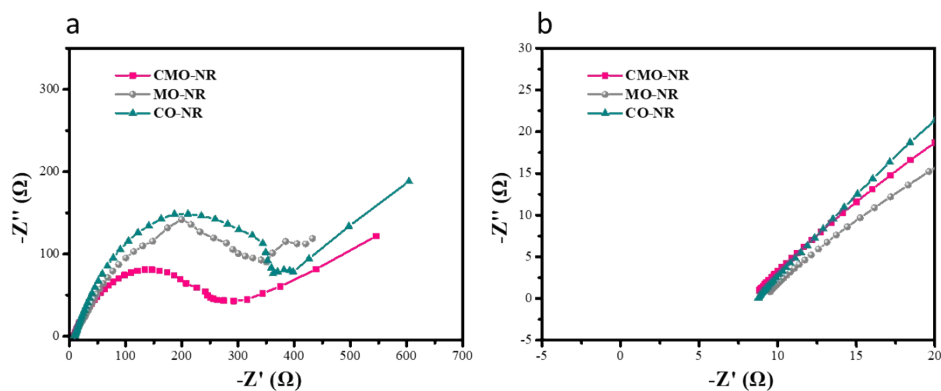


Figure S6 (a) Nyquist plots and (b) the corresponding enlarged Nyquist plots of CMO-NR, MO-NR and CO-NR.

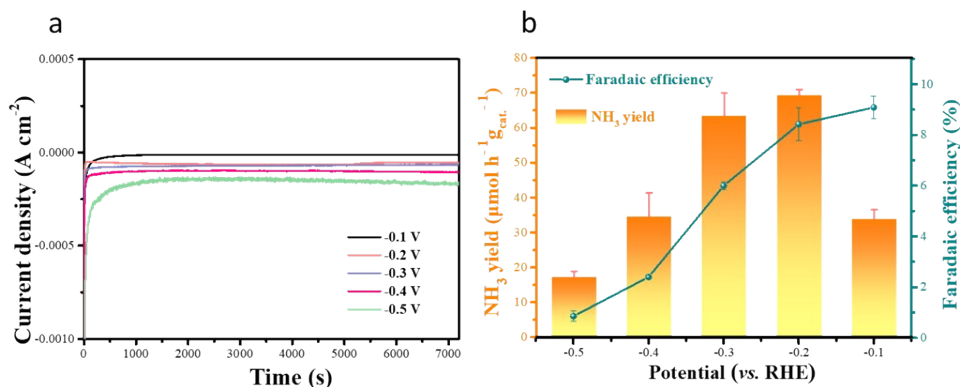


Figure S7 (a) CA curves and (b)  $\text{NH}_3$  yields and FEs of CMO-NR at different applied potentials in 0.1 M KOH.

The concentrations of  $\text{NH}_3$  in 0.1 M KOH were detected by using the indophenol blue method. The UV-vis spectroscopy and corresponding standard curves were plotted to calculate the concentrations of  $\text{NH}_3$  (Figure S2). Chronoamperometry tests were conducted on the CMO-NR at different applied potentials (-0.1 V to -0.5 V vs. RHE) during intervals of 2h, shown in Figure S7. The potentials were converted to an RHE scale according to the following equation:  $E(\text{vs. RHE}) = E(\text{vs. Hg/HgO}) + 0.865 \text{ V}$  (in 0.10 M KOH electrolyte). The corresponding CA curves in 0.1 M KOH were shown in Figure S7a, where the steady current densities increase with more negative applied potential. In Figure S7b, the average  $\text{NH}_3$  yield rate and the corresponding FE of CMO-NR were calculated.

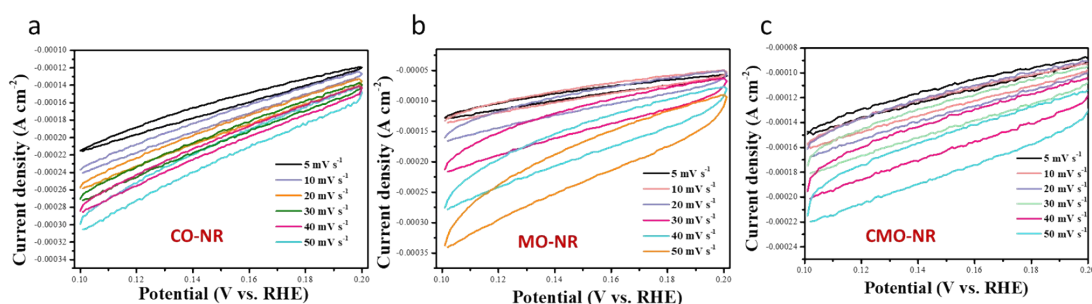


Figure S8 CV curves in the region of 0.1 to 0.2 V vs. RHE at various scan rates for (a) CO-NR, (b) Mo-NR and (c) CMO-NR catalysts.

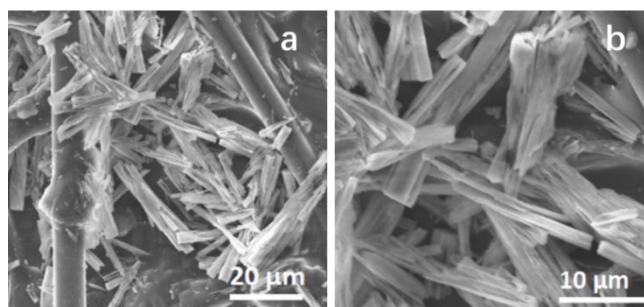


Figure S9 (a, b) SEM images of CMO-NR on carbon paper after long-term electrolysis.

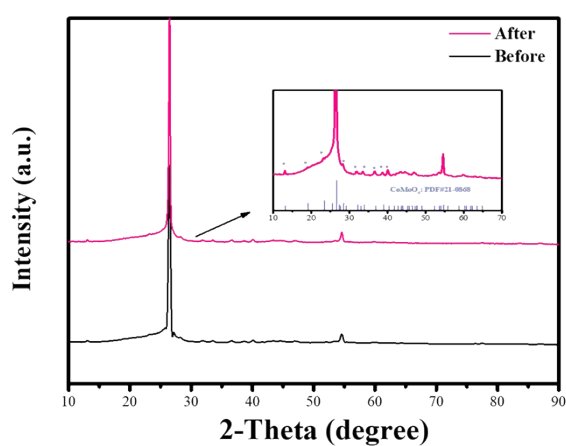


Figure S10 XRD pattern of CMO-NR on carbon paper before and after stability test.

**References:**

- 1 D. Zhu, L. Zhang, R. E. Ruther and R. J. Hamers, *Nat. Mater.*, 2013, **12**, 836–841.
- 2 G. W. Watt and J. D. Crisp, *Anal. Chem.*, 1952, **24**, 2006–2008.